Journal of
Materials Chemistry B

Materials for biology and medicine

Accepted Manuscript

This article can be cited before page numbers have been issued, to do this please use: X. Wang, F. Li, Y. Wang, C. Zhang, W. Liang, S. Shuang and C. Dong, *J. Mater. Chem. B*, 2020, DOI: 10.1039/C9TB02551K.

This is an Accepted Manuscript, which has been through the Royal Society of Chemistry peer review process and has been accepted for publication.

Accepted Manuscripts are published online shortly after acceptance, before technical editing, formatting and proof reading. Using this free service, authors can make their results available to the community, in citable form, before we publish the edited article. We will replace this Accepted Manuscript with the edited and formatted Advance Article as soon as it is available.

You can find more information about Accepted Manuscripts in the Information for Authors.

Please note that technical editing may introduce minor changes to the text and/or graphics, which may alter content. The journal's standard Terms & Conditions and the Ethical guidelines still apply. In no event shall the Royal Society of Chemistry be held responsible for any errors or omissions in this Accepted Manuscript or any consequences arising from the use of any information it contains.

ROYAL SOCIETY OF CHEMISTRY

rsc.li/materials-b

View Article Online
DOI: 10.1039/C9TB02551K

Journal Name

Visual monitoring of the lysosomal pH changes during autophagy with a red-emission fluorescent probe

Received 00th January 20xx,
Accepted 00th January 20xx

DOI: 10.1039/x0xx00000x

www.rsc.org/

Xiaodong Wang[†a], Li Fan[*†a], Yubin Wang[b], Caihong Zhang[b], Wenting Liang[a], Shaomin Shuang[b] and Chuan Dong[*a]

Autophagy play crucial roles in maintaining normal intracellular homeostasis. Molecular probes capable of monitoring lysosomal pH changes during autophagy are still highly required yet challenging to develop. Here a lysosome-targeting pH fluorescent probe **RML** is presented by introducing a methylcarbitol unit as the lysosome-targeting group to the rhodamine B, which is highly sensitive to pH changes. **RML** exhibits remarkable pH-dependent behavior at 583 nm with the fluorescent enhancement more than 148-fold. The pK_a value is determined as 4.96, and the linear response with pH changes from 4.50-5.70, which is favorable for lysosomal pH imaging. We also confirm that **RML** diffuses selectively into lysosomes using confocal fluorescent microscopy. Using **RML**, we have successfully visualized the autophagy by monitoring the lysosomal pH changes.

Introduction

Autophagy ("self-eating" in Greek) is a lysosomal degradation process for clearing dysfunctional or damaged organelles and proteins, as well as providing nutrients for cells.[1,2] Most of the widely used strategies for monitoring autophagy are based on transmission electron microscopy (TEM), and the visualization of autophagosome-related proteins by western blotting (Atg8/LC3) or genetically encoded fluorescent proteins (GFP-LC3/p62).[3-6] However, they might suffer from some inherent drawbacks. For example, they either require cell fixation (i.e. in dead cells) in the TEM and western blotting methods[7,8], or rely on complicated design and transfection process in the use of genetically encoded fluorescent proteins.[8-10] Besides, it's difficult to achieve rapid and low-cost monitoring of autophagy in live cells through these strategies.[11-13] Thus, the development of novel method for visualization of autophagy in an efficient and cost-effective manner is still highly demand.

In general, autophagy is initiated by the formation of autophagosomes, which can engulf dysfunctional organelles (such as mitochondria) or unnecessary cellular components. Subsequently, the autophagosomes fuse with lysosomes to form autolysosome, in which the cellular components are degraded by virtue of acidic hydrolase (pH 4.5-5.5).[14,15,36] Owing to inner micro-environmental difference between the lysosome and autophagosome, the lysosomal pH changes during the autophagy. Accordingly, it might be an efficient and particle method for visualization autophagy by monitoring the lysosomal pH changes.

So far, only a few pH fluorescent probes are developed for visual monitoring autophagy. Kim's group designed mitochondria-targeting pH probe for monitoring of mitochondria acidification undergoing mitophagic elimination during autophagy.[16] Unfortunately, the probe has ultraviolet excitation and short emission wavelength (no more than 550 nm), which is highly absorbed by biomolecules. Then, Iwashita designed a Mtphagy Dye with emission in the long-wavelength region, for minimizing photodamage and avoiding the influence of cell autofluorescence.[17] Shangguan's group reported a cyanine dye with red emission for simultaneously probe mitochondria and autolysosomes.[13] Although the above probes have been successfully applied in visualization of autophagy, they were both mitochondria-targetable pH probes for monitoring the pH changes of mitochondria-containing autolysosomes during the mitochondria-associated autophagy.[13,16-19] Meanwhile, the complex synthetic process and easy photobleaching of cyanine dyes may narrow their practical application. Very recently, Meng's group synthesized a benzimidazole-decorated two-photon fluorescent probe for visualization of starvation-induced autophagy via detecting pH changes in the lysosomes.[11] But the probe still has fluorescent emission within ultraviolet region. Another key issue is that the probe as well as most of the lysosome-targetable pH probes,

[a]*Institute of Environmental Science, Shanxi University, Taiyuan, 030006, P. R. China.*
[b]*College of Chemistry and Chemical Engineering, Shanxi University, Taiyuan, 030006, P. R. China.*
Email: dc@sxu.edu.cn; fanli128@sxu.edu.cn
Fax: +86-531-7011011; Tel: +86-531-7011011
[†]*These authors contributed equally to this work.*
Electronic Supplementary Information (ESI) available. See DOI: 10.1039/x0xx00000x

View Article Online
DOI: 10.1039/C9TB02551K

Journal Name

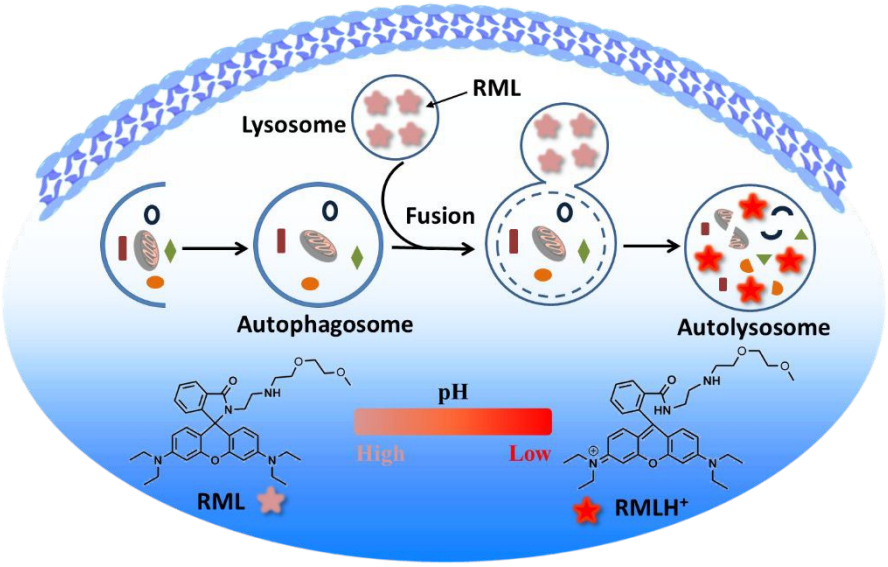

Scheme 1 Illustration of visual monitoring of autophagy utilizing the lysosome-targeting pH fluorescent probe **RML** in cells.

including the commercial LysoSensor and lysoTrackers, has weakly basic nitrogen-containing side chains (i. e. morpholine or N, N-dimethylethylenediamine) that making them selectively locate in acidic lysosomes, and would inevitably exhibit an "alkalizing effect" on lysosomes.[7, 20-28] Therefore, we aim to design novel pH probes with long-wavelength emission and negligible "alkalizing effect" on lysosomes for monitoring of autophagy by detecting the lysosomal pH changes.

RML is designed by introducing a methylcarbitol unit as the lysosome-targeting group to the rhodamine B (Scheme 1 and Scheme S1, ESI†), which is highly sensitive to pH changes due to the unique spirocycle group.[24,29-34] The spirocyclic ring usually is closed under neutral pH conditions, making rhodamine B completely nonfluorescent. Whereas protonation of N induces spirocyclic ring opening, which leads to remarkable fluorescence enhancement. Furthermore, other excellent photophysical properties including high photostability and quantum yield, together making rhodamine B suitable for long-time imaging in living cells. On the other hand, methylcarbitol is reported as a novel lysosome-targeting unit for effectively avoiding the "alkalizing effect" on lysosomes.[24] As expected, **RML** exhibits remarkable pH-dependent behavior at 583 nm with the fluorescent enhancement more than 148-fold. The pK_a value is determined as 4.96, and the linear response with pH changes from 4.50-5.70, which is favorable for lysosomal pH imaging. We also demonstrated the applicability of **RML** for visual monitoring of autophagy by imaging the lysosomal pH changes.

Results and discussion

Optical Properties of RML

The optical properties of **RML** were measured in B-R buffer solution (40 mM) containing 2.5 % DMSO for UV-vis spectra and 1 % DMSO for fluorescent spectra, respectively. As expected, the probe exhibited highly sensitive response to pH. As shown in Fig. S2 (ESI†), almost no absorption **RML** was colourless at pH 7.4. Whereas the pH reducing to 4.50, an absorbance at 561 nm is observed and increased gradually ($\varepsilon_{561\ nm}$ = 9.36 × 10^3 M^{-1} cm^{-1}), with the solution changing to pink. Fig. 1a shows the pH-dependent fluorescence spectroscopy of **RML**. Similar to the absorption spectra, there is no fluorescence observed under the near-neutral condition. Upon the pH decreasing from 7.40 to 4.40, a more than 148-fold fluorescence enhancement at 583 nm appeared (Fig. 1a). Meanwhile, the fluorescence colour of the solution turned into red under the UV lamp of 365 nm (Inset of Fig. 1a). The pK_a value was determined as 4.96, and the linear response with pH changed from 4.50-5.70, which is favourable for lysosomal pH imaging. Moreover, the fluorescence quantum yield of **RML** in B-R buffer solution increased from 0.012 to 0.214 with the pH decreasing from 7.40 to 4.40 (using rhodamine B (Φ = 0.69 in MeOH) as a reference).

To confirm the fluorescent enhancement is pH-selective, we further measured the fluorescent intensities of **RML** together with cations, anions, or amino acids at pH 7.40 and pH 4.40, respectively. No noticeable fluorescence enhancement was observed, confirming that **RML** is highly

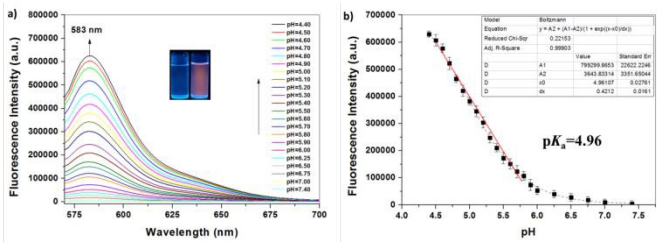

Fig. 1 (a) Fluorescence spectra changes of **RML** (10 μM) with the pH value reducing from 7.40 to 4.40 (λ_{ex} = 560 nm). Inset: the fluorescent color of **RML** changes from colorless to red with the pH decreasing. (b) Sigmoidal fitting of the fluorescence intensity at 583 nm vs pH values and the linearity relationship over the pH range from 4.50 to 5.70.

selective to pH changes and workable in biological matrixes (Fig. 2a). In addition to selectivity, we also confirmed that **RML** was high photostability (Fig. S3, ESI†), excellent reversibility against pH changes (Fig. 2b) and low cytotoxicity (Fig. S4, ESI†), respectively.

To confirm the structure-property relationship of **RML**, ^{1}H NMR-spectra at various pH values were investigated. As shown in Fig. S5 (ESI†), upon decreasing pH from 7.40 to 4.50, a distinct down-field shift is observed for the chemical shift values of the benzene ring protons (H_3, H_4 and H_5) around diethylamino and enthyl protons (H_1 and H_2) near spirocyclic ring, whereas the chemical shift values of the other protons are almost constant. These results suggest that the protonation occurs at diethylamino N atom, and further inducing spirocyclic ring opening, which results in the decrease of electron density around these protons. Thus, it is clear that the protonation of diethylamino N induces spirocyclic ring opening, leading to remarkable fluorescence enhancement.

Co-localization experiment

As reported that the methylcarbitol group has the lysosome-locating capability.[24-28] We next investigated the subcellular localization of **RML** by spatially matching the fluorescence of **RML** (10 μM) with a commercial green-emissive tracker for lysosomes, LysoTracker Green DND-26 (15 μM) in a co-localization imaging experiments. As predicted, confocal fluorescent microscopic images showed that **RML** with red

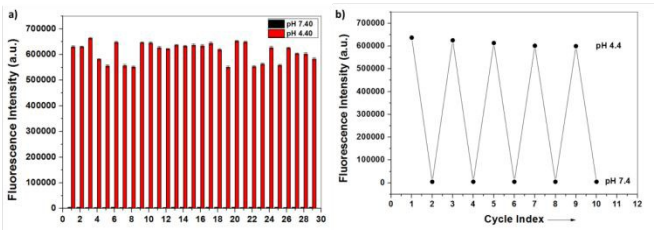

Fig. 2 (a) Selectivity of 10 μM **RML** to different potential interfering substances in 40 mM B-R buffer solution at pH 7.40 and 4.40, respectively: 1, blank; 2, K^+ (150 mM), 3, Na^+ (150 mM), 4, Mg^{2+} (2 mM), 5, Ca^{2+} (2 mM), 6, Ba^{2+} (0.2 mM), 7, Cu^{2+} (0.2 mM), 8, Fe^{2+} (0.2 mM), 9, Fe^{3+} (0.2 mM), 10, Ni^{2+} (0.2 mM), 11, Zn^{2+} (0.2 mM), 12, Cl^- (10 mM), 13, SO_4^{2-} (0.2 mM), 14, SO_3^{2-} (0.2 mM), 15, NO^- (0.2 mM), 16, Ac^- (0.2 mM), 17, H_2O_2 (0.1 mM), 18, ClO^- (0.1 mM), 19, $^1O_2$ (0.1 mM), 20, Cys (0.1 mM), 21, GSH (0.1 mM), 22, Hcy (0.1 mM), 23, Ala (0.1 mM), 24, His (0.1 mM), 25, Arg (0.1 mM), 26, Lys (0.1 mM), 27, Phe (0.1 mM), 28, Met (0.1 mM), 29, Leu (0.1 mM). (b) Fluorescence intensity changes of RML between pH 4.40 and 7.40. Conditions: λ_{ex} = 560 nm; λ_{em} = 583 nm.

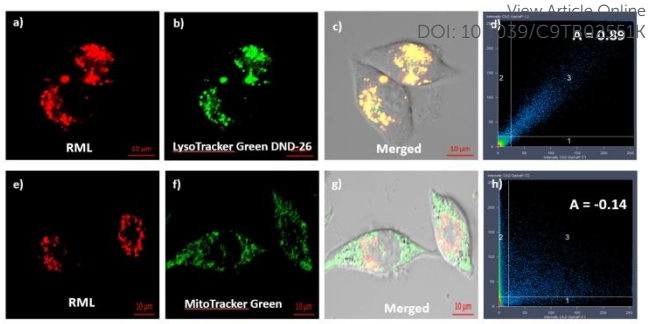

Fig. 3 Confocal microscopy fluorescence images of 10 μM **RML** (a, e) and LysoTracker Green DND-26 (15 μM) (b) and MitoTracker Green (1 μM) (f) co-stained in HeLa cells, respectively. Merged image (c, g). The correlation of **RML** with LysoTracker Green DND-26 intensities (A = 0.89) (d) and the correlation of **RML** and Mitotracker green intensities (A = -0.14) (h). The red channel image was collected at 568 - 650 nm (λ_{ex} = 561 nm) for **RML**. The green channel image was collected at 490 - 530 nm (λ_{ex} = 488 nm) for LysoTracker Green DND-26 and MitoTracker Green. Scale bar: 10 μm.

punctuated fluorescence were cell membrane permeable (Fig. 3a, e). We also calculated the logP value (n-octanol/water partition coefficient) of **RML** as 5.17 using ChemBioDraw 14.0,[24,35,36] further indicating its easy membrane permeability. More importantly, the red fluorescence image produced by **RML** (Fig. 3a, e) overlapped well with that from LysoTracker Green (Fig. 3b, c), exhibiting a Pearson's co-localization coefficient of 0.89. Meanwhile, the poor co-stained effect of probe with Mitotracker green (Fig. 3e-h) (A = -0.14) was observed. These results implied that probe can selectively accumulated in lysosomes.

Lysosome-specific intracellular pH sensing using RML

RML was further investigated for its pH-dependent fluorescence behaviour in a set of various pH high K^+ buffer with nigericin as the H^+/K^+ ionophore.[34] Almost no fluorescence could be observed at the neural condition of pH7.40 (Fig. 4a). Whereas reducing the pH to pH 4.50, the red fluorescence brightness enhanced gradually (Fig. 4b-g). In addition, **RML** also exhibited the similar pH-dependent fluorescence images in other cells such as T98G (Fig. S6, ESI†) and SMMC-7721 cells (Fig. S7, ESI†), further confirming that

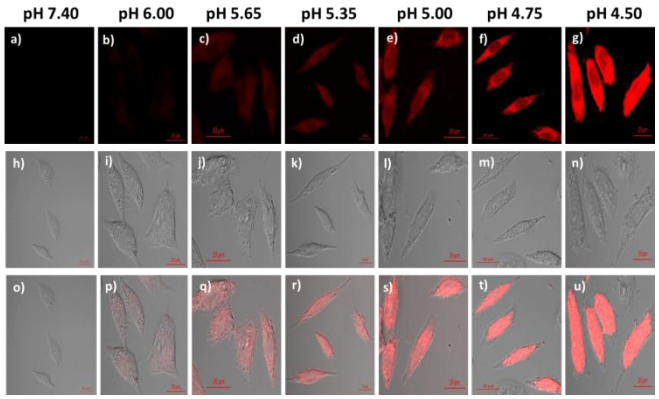

the probe could monitor the lysosomal pH

Fig. 4 Fluorescence images of HeLa cells incubated with **RML** (10 μM) at pH 7.40 (a), 6.00 (b), 5.65 (c), 5.35 (d), 5.00 (e), 4.75 (f) and 4.50 (g), respectively. (h-n) Bright-field cells images of a-g. (o-u) The corresponding merged cells images. The red emission was collected from 568 to 650 nm (λ_{ex} = 561 nm). Scale bar: 20 μm.

View Article Online
DOI: 10.1039/C9TB02557K

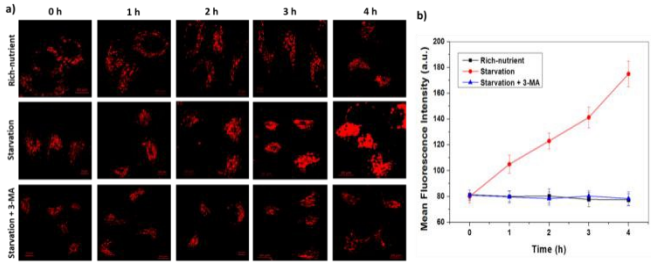

Fig. 5 Visualization of autophagy using **RML** in HeLa cells. (a) Fluorescence imaging of **RML** in HeLa cells were cultured under starvation conditions (medium of HBSS without bovine serum for inducing cell autophagy), rich-nutrient conditions (normal medium) and autophagy inhibited conditions (HBSS with 3-methyladenine (3-MA, 100 μM) for inhibiting autophagy) for a certain time (0-4 h), respectively. Cells were incubated with **RML** (10 μM) for 10 min before imaging. The red emission was collected from 568 to 650 nm (λ_{ex} = 561 nm). (b) Mean fluorescence intensity changes of a certain time (0-4 h) under different conditions (Starvation, Rich-nutrient and Starvation + 3-MA). Scale bar: 10 μm.

changes in living cells. It should be noted that the fluorescence of probe seemed to distribute throughout the whole cytoplasmic matrix, which has been observed in many previous reports.[32,34,37-39]

Visual monitoring the lysosomal pH changes during autophagy by RML

Considering that during the membrane fusion process of autophagy, the lysosomal pH in lysosomes would change due to the micro-environmental difference between the autophagosomes and lysosomes[11], we monitored the lysosomal pH changes during autophagy under starvation conditions. Herein **RML**-stained HeLa cells were cultured in Hank's Balanced Salt Solution (HBSS), a medium without nutrient to induce autophagy by starvation[11], for 0 h, 1 h, 2 h, 3 h or 4 h, respectively. As demonstrated in Fig. 5, the red fluorescence intensities enhanced gradually along with the starvation time, implying that the lysosomal pH has been decreased during the autophagy process. This might due to that the pH in autophagosomes are lower than that of lysosomes, inducing in a slight decrease of pH in the autolysosomes during the membrane fusion process of autophagy.[40-42] For comparison, the fluorescence intensities remained almost constant both under under rich-nutrient conditions (normal medium) (Fig. 5a, black line), and autophagy inhibited conditions (HBSS with 3-methyladenine (3-MA) for inhibiting autophagy) (Fig. 5b, blue line). Moreover, the red fluorescence emissions within the same field of vision in HeLa cells also enhanced along with the starvation time (Fig. S8, ESI†), further confirming that the fluorescence change of **RML** could be used as an efficient detection signal for visualization the autophagy in living cells.

Conclusion

In summary, a novel pH fluorescent probe (**RML**) was presented for visual monitoring of lysosomal pH fluctuate, by introducing methylcarbitol unit as the lysosome-targeting group to rhodamine B, which is highly sensitive to pH changes. Owing to the H^+-induced spirocyclic ring opening, **RML** exhibited a remarkable pH-dependent behavior at 583 nm with a pK_a value of 4.96. The linear response with pH changed from 4.50-5.70, which is favorable for lysosomal pH imaging. We further revealed that **RML** diffuses selectively into lysosomes and permits the visual monitoring of autophagy by detecting the lysosomal pH changes. Therefore, **RML** will be a potential imaging tool for investigating lysosome-associated physiological and pathological processes.

Experimental section

Materials and apparatus

Rhodamine B, ethylenediamine, trimethylamine, TsCl, 2-(2-methoxyethoxy)ethanol, MTT were obtained from Sigma-Aldrich. Mito Tracker Green and LysoTracker Green DND-26 were commercially available from Invitrogen. Hank's balanced salt solution (without bovine serum) was purchased from Beijing Solarbio Science & Technology Company. 3-Methyladenine were purchased from Shanghai Macklin Biochemical Company.

NMR spectra were measured on a Bruker instrument. High-resolution mass spectra was onbtaibed with a Thermo Scientific Q Exactive. pH values were acquired with a Beckman Φ50 pH meter. The UV-visible spectra measurements were obtained from a TU-1901 UV-visible spectrometer. Fluorescence spectra measurements were recorded with a FLS-920 Fluorescence Spectrometer.

Synthesis and characterization

Synthesis of Compound 1

Compound 1 was synthesized according to our previous reported.[27,28]

Synthesis of Compound 2

1.00 g (2.08 mmol) rhodamine B, 2.00 mL ethylenediamine and 1.00 mL triethylamine was mixture and refluxed in 50 mL anhydrous methanol for 24 h until the deep-red color of rhodamine B changed to deep green. The mixture was dried over anhydrous $MgSO_4$, following purified using chromatography with silica gel (CH_2Cl_2/CH_3OH, 20:1, v/v), affording a pink powder (0.94 g, 86 % yield). ^{1}H NMR ($CDCl_3$, 600 MHz) δ (ppm): 1.16-1.18 (t, 12H, -CH_3-), 2.41-2.43 (t, 2H, -CH_2-), 3.19-3.21 (t, 2H, -CH_2-), 3.32-3.36 (m, 8H, -CH_2-), 6.27-6.29 (d, 2H, Ar-H), 6.38 (s, 2H, Ar-H), 6.43-6.45 (d, 2H, Ar-H), 7.10 (m, 1H, Ar-H), 7.45 (m, 2H, Ar-H), 7.91 (m, 1H, Ar-H).

Synthesis of RML

A mixture of 0.30 g (0.62 mmol) compound 1 and 0.17 g (0.62 mmol) compound 2 was refluxed in 50 mL DMF overnight. Then mixture was dried over anhydrous $MgSO_4$, following purified using chromatography with silica gel (CH_2Cl_2), affording a light yellow powder (0.25 g, 68 % yield). ^{1}H NMR (DMSO-d_6, 600 MHz) δ (ppm): 1.11-1.13 (t, 12H, -CH_3-), 2.44 (s, 2H, -CH_2-), 2.64 (s, 2H, -CH_2-), 3.32-3.30 (m, 13H, -CH_2-), 3.47 (m, 4H, -CH_2-), 3.52 (m, 2H, -CH_2-), 6.23-6.24 (d, 2H, Ar-H), 6.34 (s, 2H, Ar-H), 6.39-6.40 (d, 2H, Ar-H), 7.03 (m, 1H, Ar-H), 7.39 (m, 2H, Ar-H), 7.85 (m, 1H, Ar-H). ^{13}C NMR

(DMSO-d_6, 150 MHz) δ (ppm): 12.56, 39.81, 44.31, 48.28, 53.51, 58.91, 65.08, 69.82, 77.13, 77.35, 77.56, 97.69, 105.16, 108.06, 122.66, 123.75, 127.98, 128.62, 130.91, 132.44, 148.70, 153.21, 153.61, 168.51. HR-MS m/z: $[M+H]^+$ calculated for $C_{35}H_{47}N_4O_4^+$, 587.3519; measured, 587.3594.

pH-dependent optical measurements

RML (1.0 mM) was dissolve in DMSO to prepare stock solution. The optical properties of **RML** were investigated in Britton-Robinson (B-R) buffer solution (acetic acid, boric acid and phosphoric acid, 40 mM) containing 2.5 % DMSO for UV-vis spectra (final concentration: 25 μM) and 1 % DMSO for fluorescent spectra (final concentration: 10 μM), respectively. Spectral data were recorded after 10 min for equilibration.

Co-localization experiments

HeLa cells were treated with **RML** (10 μM) for 10 min, then treated with LysoTracker Green DND-26 (15 μM) or Mito Tracker Green (1 μM) for additional 30 min, respectively. The fluorescence images were measured on a Laser Scanning Confocal Microscope (Zeiss, LSM880+Airyscan), with red channel (Ex = 561 nm, Em = 568 - 650 nm) for **RML**, and Green channel (Ex = 488 nm, 490 - 530 nm) for Mito Tracker Green or Lyso Tracker DND-26, respectively.

Lyso-specific intracellular pH sensing using RML

HeLa cells were first treated with **RML** (10 μM) for 10 min, then cultured in high K^+ buffer (0.5 mM $MgSO_4$, 30 mM NaCl, 120 mM KCl, 5 mM glucose, 1 mM $CaCl_2$, 1 mM NaH_2PO_4, 20 mM NaOAc and 20 mM HEPES) containing H^+/K^+ ionophore nigericin (10 μg/mL), at various pH (4.50, 4.75, 5.00, 5.35, 5.65, 6.00 and 7.40) for another 10 min, respectively.

Visual monitoring the lysosomal pH changes during autophagy using RML

HeLa cells were first treated with **RML** (10 μM) for 10 min, and then cultured under starvation conditions (HBSS without bovine serum to induce autophagy), rich-nutrient, or autophagy inhibited conditions (HBSS with 3-methyladenine (3-MA) (100 μM) to inhibit autophagy) for 0 - 4 h, respectively.

Conflicts of interest

There are no conflicts of interest to declare.

Acknowledgements

Financial supports from the National Natural Science Foundation of China (No. 21874087, 81901814 and 21976113).

Notes and references

1 S. Rodriguez-Enriquez, I. Kim, R.T. Currin and J.J. Lemasters, Autophagy., 2006, **2**, 39-46.
2 C. Settembre, A. Fraldi, D.L. Medina and A. Ballabio, *Nat. Rev. Mol. Cell Biol.*, 2013, **14**, 283-296.
3 N. Sun, D. Malide, L. Jie, I.I. Rovira, C.A. Combs and T. Finkel, *Nat. Protoc.*, 2017, **12**, 1576-1586.
4 J.M. Swanlund, K.C. Kregel and T.D. Oberley, *Autophagy.*, 2010, **6**, 270-277.
5 Y.X. Lin, Y. Wang and H. Wang, *Small.*, 2017, **13**, 1700996-1701004.
6 P. Ho¨nscheid, K. Datta and M.H. Muders, *Int. J. Radiat. Biol.*, 2014, **90**, 628-635.
7 W.J. Wang, P. Ning, Q. Wang, W. Zhang, J. Jiang, Y. Feng and X.M. Meng, *J. Mater. Chem. B.*, 2018, **6**, 1764-1770.
8 M. Li, A. Lee, K.L. Kim, J. Murray, A. Shrinidhi, G. Sung, K.M. Park and K. Kim, *Angew. Chem. Int. Ed.*, 2018, **57**, 2120-2125.
9 H.M. Ni, A. Bockus, A.L. Wozniak, K. Jones, S. Weinman, X.M. Yin and W.X. Ding, *Autophagy.*, 2011, **7**, 188-204.
10 I. Kim and J.J. Lemasters, *Am. J. Physiol. Cell. Physiol.*, 2011, **300**, C308-C317.
11 P. Ning, L.L. Hou, Y. Feng, G.Y. Xu, Y.Y. Bai, H.Z. Yu and X.M. Meng, *Chem. Commun.*, 2019, **55**, 1782-1785.
12 Y.X. Lin, S.L. Qiao, Y. Wang, R.X. Zhang, H.W. An, Y. Ma, R.P.Y.J. Rajapaksha, Z.Y. Qiao, L. Wang and H. Wang, *ACS Nano.*, 2017, **11**, 1826-1839.
13 Y. Liu, J. Zhou, L.L. Wang, X.X. Hu, X.J. Liu, M.R. Liu, Z.H. Cao, D.H. Shangguan and W.H. Tan, *J. Am. Chem. Soc.*, 2016, **138**, 12368-12374.
14 S.A. Tooze and T. Yoshimori, *Nat. Cell. Biol.*, 2010, **12**, 831-835.
15 P. Saftig and J. Klumperman, *Nat. Rev. Mol. Cell. Biol.*, 2009, **10**, 623-635.
16 M.H. Lee, N. Park, C. Yi, J.H. Han, J.H. Hong, K.P. Kim, D.H. Kang, J.L. Sessler, C. Kang and J.S. Kim, *J. Am. Chem. Soc.*, 2014, **136**, 14136-14142.
17 H. Iwashita, S. Torii, N. Nagahora, M. Ishiyama, K. Shioji, K. Sasamoto, S. Shimizu and K. Okuma, *ACS Chem. Biol.*, 2017, **12**, 2546-2551.
18 Y.C. Liu, L.L. Teng, L.L. Chen, H.C. Ma, H.W. Liu and X. B. Zhang, *Chem. Sci.*, 2018, **9**, 5347-5353.
19 L.Q. Niu, J. Huang, Z.J. Yan, Y.H. Men, Y. Luo, X.M. Zhou, J.M. Wang and J. H. Wang, *Spectrochim. Acta, Part A.*, 2019, **207**, 123-131.
20 R.P. Haugland, *Invitrogen Corp.*, 2005, 580-588.
21 F. Galindo, M.I. Burguete, L. Vigara, S.V. Luis, N. Kabir, J. Gavrilovic and D.A. Russell, *Angew. Chem., Int. Ed.*, 2005, **44**, 6504-6508.
22 H.M. Kim, M.J. An, J.H. Hong, B.H. Jeong, O. Kwon, J.Y. Hyon, S.C. Hong, K.J. Lee and B.R. Cho, *Angew. Chem., Int. Ed.*, 2008, **47**, 2231-2234.
23 X.F. Zhou, F.Y. Su, H.G. Lu, P. Senechal-Willis, Y.Q. Tian, R.H. Johnson and D.R. Meldrum, *Biomaterials.*, 2012, **33**, 171-180.
24 H. Zhu, J.L. Fan, Q.L. Xu, H.L. Li, J.Y. Wang, P. Gao and X.J. Peng, *Chem. Commun.*, 2012, **48**, 11766-11768.
25 J.T. Zhang, M. Yang, C. Li, N. Dorh, F. Xie, F. Luo, A. Tiwari and H.Y. Liu, *J. Mater. Chem. B.*, 2015, **3**, 2173-2184.
26 J.Y. Ge, L. Fan, K. Zhang, T. Ou, Y.H. Li, C.H. Zhang, C. Dong, S.M. Shuang and M.S. Wong, *Sens. and Actuators B.*, 2018, **262**, 913-921.
27 X.D. Wang, L. Fan, J.Y. Ge, F. Li, C.H. Zhang, J.J. Wang, S.M. Shuang and C. Dong, *Spectrochimica Acta Part A: Molecular and Biomolecular Spectroscopy.*, 2019, **221**, 117175-117184.
28 J.Y. Ge, K. Zhang, Li Fan, X.D. Wang, C.H. Zhang, C. Dong, M.S. Wong and S.M. Shuang, *Analyst.*, 2019, **144**, 4288-4294.
29 M. Beija, C.A. Afonso and J.M. Martinho, *Chem. Soc. Rev.*, 2009, **38**, 2410-2433.
30 Y.Q. Sun, J. Liu, X. Lv, Y. Liu, Y. Zhao and W. Guo, *Angew. Chem. Int. Ed.*, 2012, **51**, 7634-7636.
31 S.L. Shen, X.P. Chen, X.F. Zhang, J.Y. Miao and B.X. Zhao, *J. Mater. Chem. B.*, 2015, **3**, 919-925.

View Article Online
DOI: 10.1039/C9TB02551K

32 G. Niu, P. Zhang, W. Liu, M. Wang, H. Zhang, J. Wu, L. Zhang and P. Wang, *Anal. Chem.*, 2017, **89**, 1922-1929.
33 J.T. Hou, W.X. Ren, K. Li, J. Seo, A. Sharma, X.Q. Yu and J.S. Kim, *Chem. Soc. Rev.*, 2017, **46**, 2076-2090.
34 L. Fan, X.D. Wang, J.Y. Ge, F. Li, C.H. Zhang, B. Lin, S.M. Shuang and Chuan Dong, *Chem. Commun.*, 2019, **55**, 6685-6688.
35 F. Rashid, R. Horobin and M. Williams, *Histochem. J.*, 1991, **23**, 450-459.
36 G.L. Niu, R.Y. Zhang, J. P.C. Kwong, J.W.Y. Lam, C.P. Chen, J.G. Wang, Y.C. Chen, X. Feng, R.T.K. Kwok, H.H.Y. Sung, I.D. Williams, M.R.J. Elsegood, J.N. Qu, C. Ma, K.S. Wong, X.Q Yu and B.Z. Tang, *Chem. Mater.*, 2018, **30**, 4778−4787.
37 M.Y. Wu, K. Li, Y.H. Liu, K.K. Yu, Y.M. Xie, X.D. Zhou and X.Q. Yu, *Biomaterials.*, 2015, **53**, 669-678.
38 L. Cao, Z. Zhao, T. Zhang, X. Guo, S. Wang, S. Li, Y. Li and G. Yang, *Chem. Commun.*, 2015, **51**, 17324-17327.
39 Y.C. Chen, C.C. Zhu, J.J. Cen, Y. Bai, W.J. He and Z.J. Guo, *Chem. Sci.*, 2015, **6**, 3187-3194.
40 H.M. Ni, A. Bockus, A.L. Wozniak, K. Jones, S. Weinman, X.M. Yin and W.X. Ding, *Autophagy.*, 2011, **7**, 188-204.
41 H.M. Shen and N. Mizushima, *Trends Biochem. Sci.*, 2014, **39**, 61-71.
42 S.S. Li, M. Zhang, J.H. Wang, F. Yang, B. Kang, J.J. Xu and H.Y. Chen, *Anal. Chem.*, 2019, **91**, 8398-8405.

View Article Online
DOI: 10.1039/C9TB02551K

Graphical Abstract

Title: **"Visual monitoring of the lysosomal pH changes during autophagy with a red-emission pH fluorescent probe"**

Authors: *Xiaodong Wang[†], Li Fan[*†], Yubin Wang, Caihong Zhang, Wenting Liang, Shaomin Shuang and Chuan Dong[*]*

We report a red-emission pH fluorescent probe (RML) for visual monitoring of the lysosomal pH changes during autophagy in living cells.